Journal of Mathematics and Statistics 1(1): 24-28, 2005
ISSN 1549-3644

Chord Length Distributions of the Hemisphere

Wilfried Gille
Department of Physics, Martin-Luther-University Halle-Wittenberg
Hoher Weg 8, D-06120 Halle, Germany

Abstract: The distribution laws for two types of isotropic uniform random chords of the hemisphere, cap-chords and basic-chords, are investigated separately. From both distribution densities, the chord length distribution density of the whole hemisphere is derived.

Key words: μ-randomness, Shape Recognition, Scattering Experiment, Cauchy Theorem

INTRODUCTION

In material research microheterogeneities of selected materials are investigated by scattering methods. Physical structure functions, which are closely connected to the geometric covariance, result from the experiments. They allow to obtain an approximation of the chord distribution of the typical microparticles of interest. The characterization of practically all particle shapes can be completed by comparing, in each case, the experimentally obtained chord distribution with the theoretical ones, the latter requiring a large spectrum of chord distributions of geometric figures in an analytic form as compact as possible. In the present study isotropic uniform random chords in a hemisphere are investigated. Detailed explicit solutions of distribution density functions f (l) are presented.

The following methodology was applied: Two different types of random chord lengths l were simultaneously operated with. On the one hand, chords which hit the base surface of the hemisphere are considered. Independent of these, on the other hand, those chords which do not hit the basic surface are investigated likewise. Finally, the final result for all chords is obtained from these independent parts by averaging.

Chord Length Distributions: Chord length distributions result whenever a geometric figure of any dimension is randomly intersected by straight lines. The investigation of chord distribution is a special geometric matter; [1]. There exist different types of randomness for the intersection of a convex body by straight lines. Mainly three types of chords are in use. μ-chords or isotropic uniform random chords (IUR-chords) result, if the geometric figure is exposed to a uniform isotropic flow of infinite straight lines. On the other hand, the so-called weighted randomness and the two-point randomness, which are considered by Guinier and Fournet [2], are sometimes in use. All the three types are closely connected with one another, as demonstrated by Enns and Ehlers [3]. For the following exclusively μ-chords are regarded. In practice this case corresponds to the situation when an isotropic sample containing microheterogeneities with uniform shape scatters a beam of monochromatic X-ray light.

The Physical Background: There exist physical apparatuses in structure research which indirectly measure the distribution laws of random chords of a three-dimensional sample. In Small-Angle Scattering (SAS) the scattering intensity I(h) is recorded as a function of a variable h. The practical background and the theoretical foundations of this experiment are described by Guinier and Fournet [2]. From the function I(h) the so-called correlation function $\gamma(r)$ of the sample, defined by Debye and Bueche [4], which is equivalent to the set covariance K(r) of stochastic geometry, [5], can be obtained. In physics a normalization strategy of K(r) which uses the particle volume V is usual $\gamma(r) = K(r)/V$. The function $\gamma(r)$ can be calculated from $I(h)$ by the Fourier transformation:

$$\gamma(r) = \frac{\int_0^\infty h^2 \cdot I(h) \cdot \frac{\sin(h \cdot r)}{h \cdot r} dh}{\int_0^\infty h^2 \cdot I(h) dh} \qquad (1)$$

By use of $\bar{l}$ for the first moment of the distribution density $f_\mu(l)$ and $\gamma(0) = 1$, which conforms with (1), a connection between $\gamma(r)$ and $f_\mu(l)$ is obtained

$$\gamma(r) = \frac{\int_r^\infty (l - r) \cdot f_\mu(l) dl}{\bar{l}}, \quad f_\mu(l) = \bar{l} \cdot \gamma''(l). \qquad (2)$$

Some synonymous relations, well-tried in practice, follow from (1,2), Gille [6], which directly connect the functions l (h) and $f_\mu(l)$. For example

$$f_\mu(l) = \bar{l} \cdot \frac{\int_0^\infty \frac{\partial^2 \left[h^4 \cdot I(h)\right]}{\partial h^2} \cdot \frac{\sin(h \cdot l)}{h \cdot l} dh}{l^2 \cdot \int_0^\infty h^2 \cdot I(h) dh},$$

$$\bar{l} = \int_0^\infty l \cdot f_\mu(l) dl, \qquad (3)$$

holds true, if the particle system consists of two phases with different electron densities (so-called isotropic, infinitely diluted two-phase system) which, for physical reasons, can be approximated by means of an indicator function. This function equals 1 inside and 0 outside the particles. The characterization of many real particle systems can be achieved by comparing experimental chord distributions (3) with theoretical ones, provided the latter are available.

The Method Applied to the Determination of $f_\mu(l)$: For the formulation of chord length distributions different methods exist. In the cases of cylinder and parallelepiped Gille [7, 8] and for the cone Gille and Handschug [9] handled the problem by use of Theorem 1 from the publication of Enns and Ehlers [3]. This theorem formulates the distribution of the length of random secants through a convex region in terms of the intersection volume of the convex region with its translated self. This method corresponds to (2). The calculation here is based on the mere definition of the distribution function of a random chord length variable ζ, $F(l) = \Pr(\zeta < l)$. In the final step $f(l) = F'(l)$ is performed.

Fundamental Geometric Constellations: Let R be the radius of the hemisphere. The cases $0 < R < \infty$ are possible. Because of the rotational symmetry only chords $l = \overline{AB}$ whose projection $l \cdot \cos(\alpha)$ into the base plane is parallel to an invariably chosen x-axis will be considered, (Fig. 1).

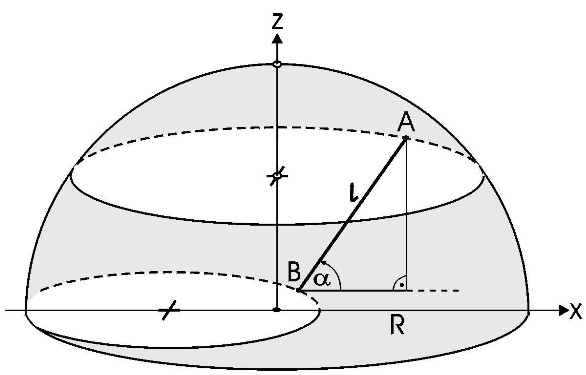

Fig. 1: The Position of a Chord l with Direction Angle in the Hemisphere Distinctly Demonstrates the Rotational Symmetry of the Problem

The possible chords will be classified into two fundamental types. For the following, chords of any length l, $0 < l < 2R$, which hit the base plane of the hemisphere are called base chords (bc), and the chords of any length l, $0 \le l \le 2R$, which exclusively intersect the cap of the hemisphere are called cap chords (cc). Because of rotational symmetry it is sufficient to consider the one random angle . The random variable is distributed with density cos( ) on the interval $0 \le \alpha \le \pi/2$. The concrete interval limits depend on l, see Table 1.

Table 1: The Fundamental Limits of the Direction-angle

Case 1:	$0 \le l \le R$	$0 \le \alpha \le \pi/2$
Case 2:	$R \le l \le \sqrt{2}R$	$0 \le \alpha \le \arcsin(R/l)$
Case 3:	$\sqrt{2}R < l \le 2R$	$0 \le \alpha \le \arccos(l/(2R))$

Within these intervals a further interval-splitting of cases 1 and 2 is essential, if concrete integrals for averaging over are evaluated. The probability $F(l) = \Pr(\zeta < l)$ is expressed by ratios of projection-portions perpendicular to the direction . For the moment, for a constant the whole projection area being "possible" in terms of probability is subdivided into two parts, Fig. 2. For bc the "possible" area $S_{bc}(\alpha)$ perpendicular to the chord direction follows from

$$S_{bc}(\alpha) = \pi \cdot R^2 \cdot \sin(\alpha). \tag{4}$$

The complementary part $S_{cc}(\ )$ of the projection area perpendicular to direction for the cc is

$$S_{cc}(\alpha) = \frac{\pi \cdot R^2}{2} - \frac{\pi \cdot R^2}{2} \cdot \sin(\alpha). \tag{5}$$

After averaging over the angle from (4,5) one obtains

$$\bar{S}_{bc} = \int_0^{\frac{\pi}{2}} S_{bc}(\alpha) \cdot \cos(\alpha) d\alpha = \frac{\pi}{2} \cdot R^2,$$

$$\bar{S}_{cc} = \int_0^{\frac{\pi}{2}} S_{cc}(\alpha) \cdot \cos(\alpha) d\alpha = \frac{\pi}{4} \cdot R^2. \tag{6}$$

Thus, the sum of the two mean projection areas in (6) is $(3/4) \cdot \pi R^2$, which coincides with the general theorem according to which the mean projection plane of any convex geometric figure equals one quarter of its whole surface [10].

$$\bar{S}_p = \frac{S}{4} \tag{7}$$

Therefore, the ratio of the measures of bc and cc equals 2:1, which will be used for considering all μ-chords of the hemisphere,

$$F_\mu(l) = \frac{1}{3} \cdot F_{\mu cc}(l) + \frac{2}{3} \cdot F_{\mu bc}(l) \tag{8}$$

Determination of the Favorable Projection-area Shares: According to Table 1, a constant l is considered. The probabilities $F_{\mu bc}(l)$ and $F_{\mu cc}(l)$

correspond to exactly those parts of the projecting areas (6) which guarantee $\zeta < l$. These areas can generally be determined by formal integration in the following way: Let $A(R,l,\alpha)$ be the area share within the basic circle of the hemisphere which cannot be reached by the lower end of any bc of length ζ with fixed direction under the condition ζ<l. Evidently $A(R,l,\alpha)$ represents the common overlapping area of the two circles

$$x^2+y^2=R^2,\ \left(x+l\cdot\cos(\alpha)\right)^2+y^2=R^2-l^2\cdot\sin^2(\alpha)$$

in the base plane, where the smaller circle can lie completely within the greater one. The distribution function $F_{\mu bc}$ can be expressed by use of (6)

$$F_{\mu bc}(l)=\frac{\frac{\pi}{2}\cdot R^2-\int_0^{\alpha_{max}}A(R,l,\alpha)\cdot\cos(\alpha)\cdot\sin(\alpha)d\alpha}{\frac{\pi}{2}\cdot R^2} \tag{9}$$

The factor cos( ) in (9) is the IUR-factor, and analogously to (4) the factor sin( ) transforms the area share from the basic plane into a direction perpendicular to the bc. The integration limits in (9) must be specified for each l-interval in Table 1. Moreover, the integral in (9) in case 1 and 2 must additionally be split into two parts. This phenomenon is similar to the interval-splitting in the different cone-cases, as explained by Gille and Handschug [9].

In case 1 the intervals $0\le\alpha\le\arccos\left(l/(2R)\right)$ and $\arccos\left(l/(2R)\right)\le\alpha\le\pi/2$ must be distinguished. Finally, in case 2 the intervals $0\le\alpha\le\arccos\left(l/(2R)\right)$ and $\arccos\left(l/(2R)\right)\le\alpha\le\arcsin(R/l)$ must be considered. In the cc-case it is simpler to express the probability $F_{\mu cc}(l)$ by use of (6) already at the beginning by an area $F(R,l,\alpha)$ which lies perpendicular to the -direction,

$$F_{\mu cc}(l)=\frac{\frac{\pi}{4}\cdot R^2-\int_0^{\arccos(l/(2R))}F(R,l,\alpha)\cdot\cos(\alpha)d\alpha}{\frac{\pi}{4}\cdot R^2} \tag{10}$$

In (10) $F(R,l,\alpha)$ is half the area limited by an ellipse with semiaxes R and $R\cdot\sin(\alpha)$ and a circle with radius $r=\sqrt{R^2-l^2/4}$ with the same centre.

Hereby, $F(r,l,\alpha)$ is the area within the circle but outside the ellipse, Fig. 2. The first derivative of $F(R,l,\alpha)$ with respect to l is

$$\frac{\partial F(R,l,\alpha)}{\partial l}=-\frac{l}{2}\cdot\arccos\left(\frac{\tan(\alpha)}{\sqrt{\frac{4R^2}{l^2}-1}}\right) \tag{11}$$

which can be used for the differentiation of the parametric integral (10) with respect to l. The area-parts $A(R,l,\alpha)$ and $F(R,l,\alpha)$ correspond to the $l-\alpha-$ intervals and follow from pure geometry.

Details of the integration and differentiation strategy are omitted here. The calculation of the antiderivatives and derivatives of the integrals (9,10) is troublesome.

The Resulting Distribution Densities: The final results are surprisingly simple. Certain abbreviations (12) are expedient:

$$\begin{cases} p=\sqrt{\frac{4R^2}{l^2}-1} \\ q=\sqrt{4-\frac{l^2}{R^2}} \\ a=-\frac{l}{\pi\cdot R^2}\cdot\arctan(p)-\frac{R^2}{\pi\cdot l^3}\cdot\arctan\left(\frac{p}{\frac{2R^2}{l^2}-1}\right) \\ b=p\cdot\left(2l^4+l^2R^2+6R^4\right)+q\cdot\left(8lR^3-2Rl^3\right) \end{cases} \tag{12}$$

For bc

$$f_{\mu bc}(l)=\begin{cases} \left(b+12\pi l^2R^2\right)/\left(12\pi lR^4\right)+a, & 0<l\le R \\ 1/\left(12\pi lR^4\right)\cdot\left(b+12\pi R^6/l^2\right)+a, & R\le l\le\sqrt{2}\cdot R \\ b/\left(12\pi lR^4\right)+a, & \sqrt{2}\cdot R\le l\le 2\cdot R \\ 0, & 2\cdot R\le l<\infty \end{cases} \tag{13}$$

holds. For the cc,

$$f_{\mu cc}(l)=\begin{cases} 2l/\left(\pi R^2\right)\cdot\arctan(p), & 0\le l\le 2R \\ 0, & 2R\le l<\infty \end{cases} \tag{14}$$

holds. If all the bc and cc are considered, $f_\mu(l)$ follows by use of (8). Finally, the simplification of the resulting expressions in all l-intervals yields:

Journal of Mathematics and Statistics 1(1): 24-28, 2005
ISSN 1549-3644

$$f_\mu(l)=\begin{cases} 2l/\left(3R^2\right)-\left(4R^2\cdot\arcsin\left(l/(2R)\right)\right)/\left(3\pi l^3\right)+ & \\ \sqrt{1-l^2/\left(4R^2\right)}\cdot\left(1/(\pi R)+2R/\left(3\pi l^2\right)\right), & 0\le l\le R \\ \sqrt{1-l^2/\left(4R^2\right)}\cdot\left(1/(\pi R)+2R/\left(3\pi l^2\right)\right)+\left(4R^2\cdot\arccos\left(l/(2R)\right)\right)/\left(3\pi l^3\right), & R\le l\le 2R \\ 0, & 2R<=l<\infty \end{cases} \tag{15}$$

Beside the field of SAS, applications of (11-15) are important to the acoustical design of auditory, nuclear fuels, automatic pattern recognition, so-called mean free path problems and absorption problems of any radiation concerning hemisphere geometries. Figure 3 shows the results for the standard R=1.

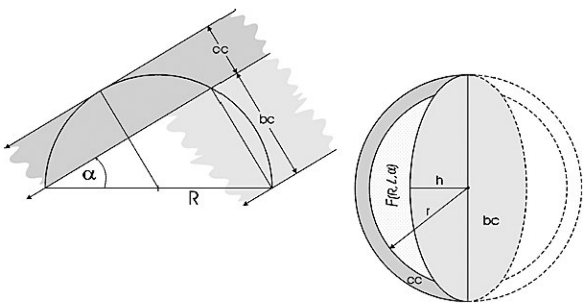

Fig. 2: For Each , $0\le\alpha\le\pi/2$, There Exist bc and cc. For a Constant the bc Area and the cc Area are Limited by an Ellipse with Semiaxes R and $h=R\cdot\sin(\alpha)$

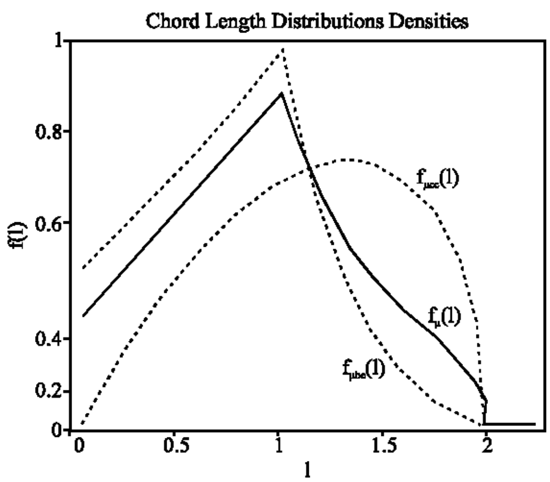

Fig. 3: The Functions $f_{\mu bc}(l)$, and $f_{\mu cc}(l)$ and $f_\mu(l)$ are Continuous in the Whole l-interval, $0\le l<\infty$. However, $f_{\mu bc}'(l)$ and $f_\mu'(l)$ are Discontinuous at l=R. The Derivatives $f_{\mu cc}'(l)$ and $f_\mu'(l)$ are Discontinuous at $l=2\cdot R$

Distinctive Properties of the Resulting Densities: Contrary to the sphere, cone and parallelepiped the functions (11-15), including their first derivatives, are continuous in $0<l<2R$, and particularly, too, at the transition positions l=R and $l=\sqrt{2}\cdot R$.

In the case $l\to 0$, $f_{\mu cc}(0)=0$ holds and therefore $f_\mu(0+)=(2/3)\cdot f_{\mu bc}(0+)$ is obtained. The final result is

$$f_\mu(0+)=\frac{8}{9\pi\cdot R}.$$

The essential result as to the data evaluation in SAS is $f_\mu(l)$ for $l_{min}<l$. Particularly a particle system, consisting of hemispheres which all coincide in R, should lead to an experimental chord distribution (3). The largest particle dimension L=2R can be determined precisely from the left-side derivative of $f_\mu(2R)$, which equals $-\infty$. Hence the position l=2R is clearly marked. This detail extremely differs from the behaviour obtained for other geometric figures, Fanter [11]. The global maximum of $f_\mu(l)$ lies at the position l=R. Further the position $l=\sqrt{2}\cdot R$ is an interesting one. The corresponding density-values are

$$f_\mu(R)=\frac{15\sqrt{3}+8\pi}{18\pi\cdot R},\quad f_\mu\left(\sqrt{2}R\right)=\frac{8+\pi}{6\sqrt{2}\cdot\pi\cdot R}. \tag{16}$$

The right-side and the left-side derivatives $f_\mu'(R\pm)$ are

$$f_\mu'(R\pm)=\frac{-25\sqrt{3}\mp 24\pi}{18\pi\cdot R^2}.$$

The first two derivatives of $f_\mu(l)$ at $l=\sqrt{2}\cdot R$ are the following:

$$f_\mu'\left(\sqrt{2}\cdot R\right)=-\frac{16+3\pi}{12\pi\cdot R^2},\quad f_\mu''\left(\sqrt{2}\cdot R\right)=\frac{\sqrt{2}(2+\pi)}{2\pi\cdot R^3} \tag{17}$$

From (16,17) follows the fact that the position $l=l_i$ of a point of inflexion of $f_\mu(l)$ lies in the interval $\sqrt{2}\cdot R<l_i<2\cdot R$. The theoretical relations for the moments of $f_\mu(l)$, $M_0=1$, $M_1=4V/S$ and

$M_4 = 12 \cdot V^2 / (\pi \cdot S)$ are fulfilled. The second moment M_2 equals R^2.

For more information, please contact the author. Programs and files for all steps of the calculation project are available.

REFERENCES

1. Stoyan, D., W.S. Kendall and J. Mecke, 1987. Stochastic geometry and its applications. Akademie-Verlag, Berlin.
2. Guinier, A. and G. Fournet, 1955. Small-angle Scattering of X-rays. Wiley, New York.
3. Enns, E.G. and P.F. Ehlers, 1978. Random paths through a convex region. J. Applied Probability, 15: 144-152.
4. Debye, P. and A.M. Bueche, 1949. Scattering by an inhomogeneous solid. J. Applied Physics, 20: 518-525.
5. Serra, J., 1982. Image Analysis and Mathematical Morphology. Academic Press, London.
6. Gille, W., 1994. The integrals of small-angle scattering and their calculation. J. Physique, IV/I, 3-C8 : 503-506.
7. Gille, W., 1988. The chord length distribution density of parallelepipeds with their limiting cases. Experimentelle Technik der Phys., 36: 197-208.
8. Gille, W., 2000. Chord length distributions and small-angle scattering. The European Physical J., B17: 371-383.
9. Gille, W. and H. Handschug, 1999. Chord length distribution density and small-angle scattering correlation function of the right circular cone. Mathematical and Computer Modelling 30: 107-130.
10. Kendall, M. G. and P.A.P. Moran, 1963. Geometric Probability, Griffin, London.
11. Fanter, D., 1973. Modelluntersuchungen zur Auswertung von Roentgenstreukurven mittels eines Fourier-Verfahrens. Ph.D. Thesis. Institut fuer Polymerchemie, Berlin Teltow-Seehof.